

Relaxor-like dynamics of ferroelectric $\text{K}(\text{Ta}_{1-x}\text{Nb}_x)\text{O}_3$ crystals probed by inelastic light scattering

M. M. Rahaman, T. Imai, J. Miyazu, J. Kobayashi, S. Tsukada, M. A. Helal, and S. Kojima

Citation: *Journal of Applied Physics* **116**, 074110 (2014); doi: 10.1063/1.4893363

View online: <http://dx.doi.org/10.1063/1.4893363>

View Table of Contents: <http://scitation.aip.org/content/aip/journal/jap/116/7?ver=pdfcov>

Published by the AIP Publishing

Articles you may be interested in

Temperature dependent Raman scattering and far-infrared reflectance spectra of MgO modified $\text{Pb}_{0.99}(\text{Zr}_{0.95}\text{Ti}_{0.05})_{0.98}\text{Nb}_{0.02}\text{O}_3$ ceramics: A composition effect

J. Appl. Phys. **116**, 093513 (2014); 10.1063/1.4894467

Broadband inelastic light scattering study on relaxor ferroelectric $\text{Pb}(\text{In}_{1/2}\text{Nb}_{1/2})\text{O}_3\text{-Pb}(\text{Mg}_{1/3}\text{Nb}_{2/3})\text{O}_3\text{-PbTiO}_3$ single crystals

J. Appl. Phys. **115**, 234103 (2014); 10.1063/1.4878855

Phase transition behaviors in relaxor ferroelectric [001]-poled $\text{Pb}(\text{In}_{1/2}\text{Nb}_{1/2})\text{O}_3\text{-Pb}(\text{Mg}_{1/3}\text{Nb}_{2/3})\text{O}_3\text{-PbTiO}_3$ single crystals studied by Brillouin light scattering and dielectric spectroscopies

J. Appl. Phys. **111**, 054103 (2012); 10.1063/1.3692596

Order-disorder behavior of ferroelectric phase transition of $\text{KTa}_{1-x}\text{Nb}_x\text{O}_3$ probed by Brillouin scattering

Appl. Phys. Lett. **98**, 092909 (2011); 10.1063/1.3560345

Light scattering from $(\text{K}_{0.5}\text{Na}_{0.5})_{0.2}(\text{Sr}_{0.75}\text{Ba}_{0.25})_{0.9}\text{Nb}_2\text{O}_6$ with the tungsten bronze structure: An analogy with relaxor ferroelectrics

J. Appl. Phys. **89**, 1671 (2001); 10.1063/1.1337923

2014 Special Topics



PEROVSKITES



2D MATERIALS



MESOPOROUS MATERIALS



BIOMATERIALS/
BIOELECTRONICS



METAL-ORGANIC
FRAMEWORK
MATERIALS



Submit Today!

Relaxor-like dynamics of ferroelectric $\text{K}(\text{Ta}_{1-x}\text{Nb}_x)\text{O}_3$ crystals probed by inelastic light scattering

M. M. Rahaman,^{1,a)} T. Imai,² J. Miyazu,² J. Kobayashi,² S. Tsukada,³ M. A. Helal,¹ and S. Kojima^{1,b)}

¹Graduate School of Pure and Applied Sciences, University of Tsukuba, Tsukuba, Ibaraki 305-8573, Japan

²NTT Photonic Laboratories, Nippon Telegraph and Telephone Corporation, Atsugi, Kanagawa 243-0198, Japan

³Faculty of Education, University of Shimane, Matsue, Shimane 690-8504, Japan

(Received 22 May 2014; accepted 5 August 2014; published online 20 August 2014)

The relaxor-like dynamics of the cubic-tetragonal ferroelectric phase transition was studied by Brillouin and Raman scattering in $\text{K}(\text{Ta}_{1-x}\text{Nb}_x)\text{O}_3$ (KTN) crystals with $x = 0.40$ (KTN40). The local symmetry breaking by the polar nanoregions (PNRs) was observed in a paraelectric phase by Raman scattering on the $A_1(z)$ mode of the PNRs with $R3m$ symmetry. Upon cooling from a high temperature, the remarkable increase in the LA phonon damping starts at 45 K above the cubic-tetragonal phase transition temperature of $T_{\text{C-T}} = 308$ K, which is defined as the intermediate temperature, $T^* \sim 353$ K, indicating the start of the rapid growth of the PNRs. The coupling between the LA mode and fluctuation of the PNRs caused a remarkable elastic anomaly in the vicinity of $T_{\text{C-T}}$. The analysis of the temperature dependent central peak shows a critical slowing down towards $T_{\text{C-T}}$, which is the evidence for the order-disorder nature of a ferroelectric phase transition. The evolution of the dynamic PNRs is discussed by the estimation of their length scale, and it is found that it starts to increase near T^* and gradually grows towards $T_{\text{C-T}}$. © 2014 AIP Publishing LLC.

[<http://dx.doi.org/10.1063/1.4893363>]

I. INTRODUCTION

The lead-based relaxor ferroelectrics (RFEs) have attracted much attention due to their significant piezoelectricity and high dielectric response. Thus, the developments of lead free ferroelectric materials are the urgent topic in applied physics due to adverse environmental effect of lead. Among them potassium tantalate niobate, $\text{KTa}_{1-x}\text{Nb}_x\text{O}_3$ (abbreviated KTN100x) is of particular interest in its technological importance for optical applications due to its high quadratic electro-optic coefficient and excellent photorefractive effect.¹ A recent study of the acoustic emission of a high quality KTN32 ($x = 0.32$) single crystal shows a relaxor-like behavior by observation of the Burns temperature, $T_{\text{B}} \sim 620$ K, at which polar nanoregions (PNRs) appear, and the intermediate temperature, $T^* \sim 310$ K, indicating the start of the PNRs rapid growth.² Such a relaxor-like behavior was observed even in the normal ferroelectric BaTiO_3 .³ Based on comparison with lead-based RFEs, which are highly complex, presenting both a chemical and structural local order, KTN exhibits relaxor-like properties, but much less complicated than the lead-based RFEs.^{4,5} Moreover, the central peak (CP), a common feature of the order-disorder phase transition, coexists with the soft mode, a general property of the displacive phase transition, in the KTN single crystals.⁶ Therefore, KTN is better suited for the investigation of the fundamental origin and mechanism of the relaxor-like behavior.

The KTN crystals are solid solutions of potassium tantalate and potassium niobate. Its end member of KTaO_3

displays a quantum paraelectricity and retains a cubic symmetry down to 0 K by quantum fluctuations. In KTN, Nb ions that replaces Ta ions go off-center in the B-site, and they induce the local polarizations.⁷ The off-centering of Nb was described by an eight site model in which the Nb ions move among the equivalent eight [111] directions.⁸ The off-center displacement of Nb ions in the KTN was accurately determined by X-ray absorption fine-structure measurements.⁷ The different types of measurements, such as acoustic emission,² infrared absorption,⁹ Raman scattering,^{6,10} Brillouin scattering,¹¹ as well as refractive index and linear-birefringence¹² were investigated to clarify the dynamics of the PNRs in the cubic phase. To the best of our knowledge, no result was reported regarding to the local symmetry of PNRs, which are the physical origin of the elastic anomalies and critical slowing down in high quality KTN single crystals. In spite of many experimental and theoretical efforts carried out to date, the exact knowledge of the static and dynamic features of the PNRs is far from completely understood. The main parameter of understanding the cubic-tetragonal phase transition behavior is the dynamic properties related to the temperature evolution of the dynamic and static PNRs. The static PNRs appear below T^* , and the rapid growth of PNRs occurs. Therefore, it is important to study the dynamic properties of KTN to clarify the nature of the ferroelectric phase transition and the dynamics of the PNRs. In the present study, the local symmetry breaking in the PNRs was studied by Raman scattering in a paraelectric phase of the KTN40 ($x = 0.40$) crystals. The dynamics of the PNRs were studied by Brillouin scattering to clarify the elastic anomaly in the GHz range caused by the coupling of acoustic phonons with the PNRs and their slowing down.

^{a)}Electronic mail: mijan_mse@ru.ac.bd

^{b)}Electronic mail: kojima@ims.tsukuba.ac.jp

II. EXPERIMENT

KTN40 single crystals grown by the top seeded solution growth method (TSSG)¹³ were cut into $4 \times 3.2 \times 1 \text{ mm}^3$ size pieces along the a , b , and c axes in the cubic coordinate system. The largest (100) surfaces of the crystal were polished to optical grade. The Brillouin scattering was excited at 532 nm from a single frequency solid state laser and measured by a Sandercock-type 3 + 3 passes tandem Fabry-Perot interferometer at a back scattering geometry.¹⁴ The free spectral ranges (FSR) of the spectrometer were fixed at 75 GHz for the longitudinal acoustic (LA), transverse acoustic (TA) mode and at 300 GHz for the CP measurements. The Raman scattering was excited at 532 nm from a single frequency solid state laser. The scattered light was collected at the back scattering geometry and analyzed by a triple grating spectrometer (Jobin Yvon, T64000) with the resolution of 2 cm^{-1} . The temperature of the sample was regulated by a heating/cooling stage (Linkam, THMS600) with the temperature stability of $\pm 0.1 \text{ K}$ over the entire temperature range.

III. RESULTS AND DISCUSSION

A. Local symmetry breaking observed by Raman scattering

Raman scattering of KTN40 was measured as a function of temperature to study the local symmetry breaking in the cubic phase. Recently, Raman scattering of the typical relaxor, $\text{Pb}(\text{Zn}_{1/3}\text{Nb}_{2/3})\text{O}_3$ - PbTiO_3 (PZN-PT), with a perovskite structure was studied in the cubic phase to clarify the local symmetry breaking due to the existence of PNRs with a rhombohedral $R3m$ symmetry.^{15,16} Figure 1 shows the typical Raman spectra observed in the $a(bc)\bar{a}$ (VH) back scattering geometry at selected angles rotated along the a -axis, where 0° means the scattering geometry of $a(bc)\bar{a}$. The inset shows the spectrum between 400 and 730 cm^{-1} fitted by the damped harmonic oscillator (DHO) function. The dotted ($\sim 470 \text{ cm}^{-1}$) and dashed ($\sim 575 \text{ cm}^{-1}$) bands denote the modes of second order scattering, whereas the solid band ($\sim 540 \text{ cm}^{-1}$) indicates the first order scattering of the TO_4 mode.¹⁷ The temperature dependence of the intensity of the TO_4 mode was measured in the vicinity of $T_{\text{C-T}}$. Above $T_{\text{C-T}}$, the first order TO_4 peak still appeared. According to the

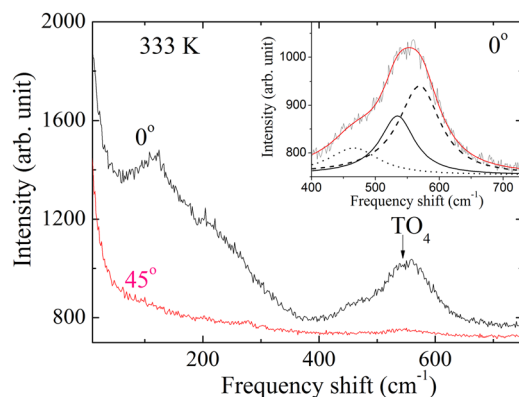


FIG. 1. $a(bc)\bar{a}$ Raman spectra of KTN40 at two selected rotation angles in a cubic symmetry.

Raman selection rule, this mode is Raman inactive in the cubic phase with $Pm\bar{3}m$ symmetry. The temperature dependence of the peak intensity is shown in Fig. 2(b). In the cubic phase, the weak intensity of the TO_4 mode still remains by the local symmetry breaking in the dynamic PNRs with a rhombohedral symmetry. In order to clarify the symmetry breaking caused by the PNRs, we analyzed the angular dependence of the VH spectra in the paraelectric phase as shown in Fig. 2(a). In particular, we were mainly concerned about the TO_4 mode, and the intensity of this mode clearly showed the peak variation, which is similar to the behavior of the PNRs.¹⁸

According to the neutron pair distribution function analysis, the symmetry of the PNR of $\text{Pb}(\text{Mg}_{1/3}\text{Nb}_{2/3})\text{O}_3$ (PMN) was $R3m$.¹⁹ For $R3m$ symmetry, there are three Raman active modes, $A_1(z)$, $E(y)$ and $E(-x)$ with the following Raman tensors:¹⁸

$$A_1(z) = \begin{pmatrix} a & 0 & 0 \\ 0 & a & 0 \\ 0 & 0 & b \end{pmatrix} \quad E(y) = \begin{pmatrix} c & 0 & 0 \\ 0 & -c & d \\ 0 & d & 0 \end{pmatrix}$$

$$E(-x) = \begin{pmatrix} 0 & -c & -d \\ -c & 0 & 0 \\ -d & 0 & 0 \end{pmatrix}.$$

The angular dependence was calculated using the following expression:¹⁸

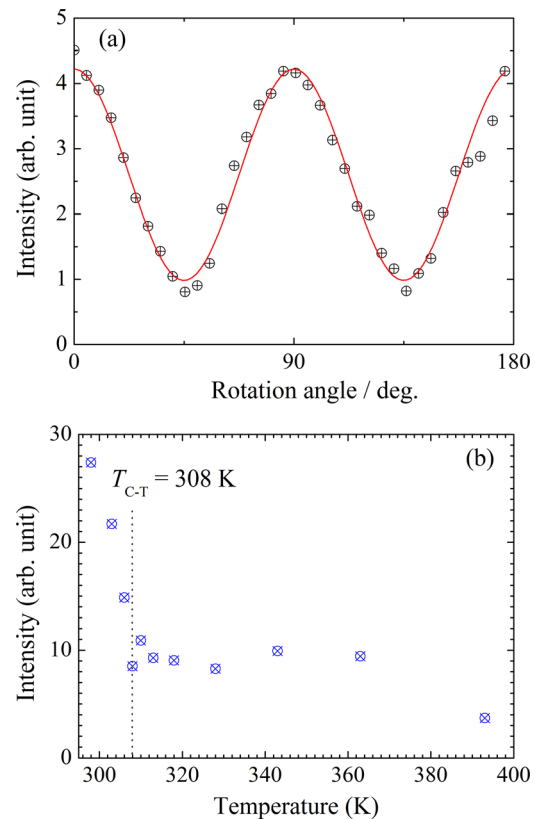


FIG. 2. (a) The angular dependence of the TO_4 mode intensity, where the observed intensity is denoted by the open symbols. The solid line denotes the calculated intensity of the $A_1(z)$ mode of the PNRs. (b) Temperature dependence of the TO_4 mode intensity at 0° .

$$\vec{R}^{-1} \cdot \vec{C}^{-1} \cdot (A_1(z) \text{ or } E(y) \text{ or } E(-x)) \cdot \vec{R} \cdot \vec{C}, \quad (1)$$

where

$$\vec{R} = \begin{pmatrix} 1 & 0 & 0 \\ 0 & \cos \theta & -\sin \theta \\ 0 & \sin \theta & \cos \theta \end{pmatrix}$$

and \vec{C} is the transformation matrix corresponding to Raman tensor modification.¹⁸ Since the local rhombohedral regions are randomly oriented with eight equivalent polarization directions, we calculated the angular dependence in the multi-domain states in which the contributions of all the domains are equally summed up.¹⁸ The angular dependence of the TO₄ mode intensity is plotted by the open circles in Fig. 2(a). The observed data were fitted using the *bc* components of Eq. (1) for *A₁(z)* mode. The fitted curve reproduces the observed intensity variation revealing that the TO₄ mode in the paraelectric phase stems from the *A₁(z)* mode of the PNRs with a rhombohedral *R3m* symmetry. Therefore, in the cubic symmetry, the KTN is considered to be composed of at least locally distorted PNRs with *R3m* in the cubic matrix with *Pm3m* symmetry below the Curie temperature. The detailed Raman results of KTN40 will be separately published.

B. Acoustic anomaly and central peak

The Brillouin scattering spectra of FSR = 75 GHz observed at selected temperatures are shown in Fig. 3(a). Each spectrum consists of doublet peaks of the LA and TA modes. In the broadband spectra of FSR = 300 GHz, a CP was observed as shown in Fig. 3(b). The breaking of Brillouin selection rule is clearly revealed by TA mode which is inactive in cubic symmetry at the back scattering geometry.²⁰ The TA mode above the Curie temperature was not only in the present KTN crystals grown in NTT but also in the KTN crystals grown in MTI, USA. Therefore, it is certain that the TA mode appears at least in the composition range $x = 0.3 \sim 0.4$. In Raman scattering, the first order scattering is forbidden in a cubic phase, while the scattering intensity of the first order still remains strongly above T_{C-T} . We ascribed the origin of local symmetry breaking to PNRs with high number density.

The frequency shift, Δv_B , is related to the phase velocity, V , of a sound wave by Eq. (2)¹⁴

$$\Delta v_B = \pm \frac{2nV}{\lambda_0} \sin\left(\frac{\theta}{2}\right), \quad (2)$$

where λ_0 , n , and θ are the wavelength of the incident light, refractive index of the observed sample, and scattering angle, respectively. The LA and TA sound velocities determined from the frequency shifts of the LA and TA peaks are shown in Figs. 4(a) and 4(b). The observed LA and TA sound velocities are related to the elastic constants C_{11} and C_{44} in a cubic coordinate, respectively.²⁰ The LA velocity shows a remarkable softening in the vicinity of the cubic-tetragonal ferroelectric phase transition temperature, $T_{C-T} = 308$ K, while the TA velocity shows only a slight softening and a small

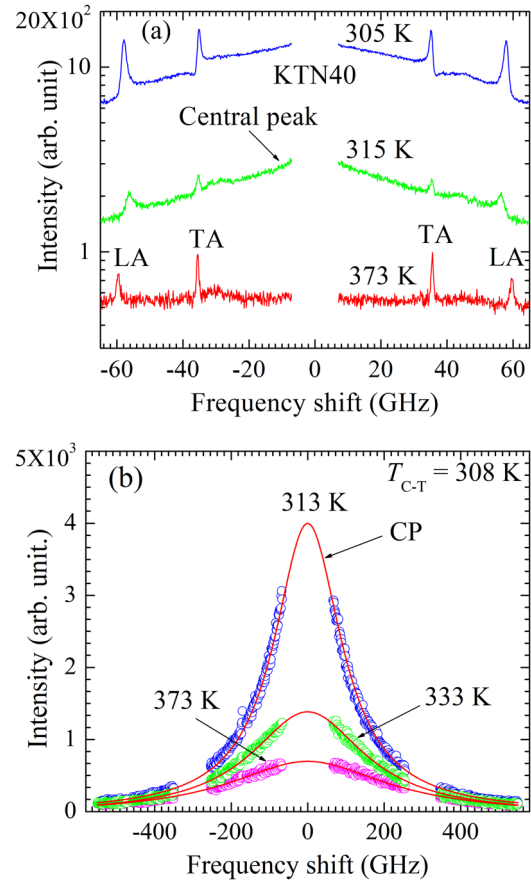


FIG. 3. Brillouin scattering spectra at selected temperatures of a KTN40 single crystal measured with the FSR (a) 75 GHz and (b) 300 GHz. The solid lines in (b) indicate the curves fitted by the Voigt function.

discontinuity at T_{C-T} , reflecting the nature of a slightly first order phase transition. The softening of the LA velocity near the Curie temperature and marked increase in the sound attenuation were observed in various lead-based perovskite relaxors, such as 0.65Pb(Mg_{1/3}Nb_{2/3})O₃–0.35PbTiO₃ (PMN-35PT), 0.70Pb(Sc_{1/2}Nb_{1/2})O₃–0.30PbTiO₃ (PSN-30PT), 0.85Pb(Zn_{1/3}Nb_{2/3})O₃–0.15PbTiO₃ (PZN-15PT), 0.65Pb(In_{1/2}Nb_{1/2})O₃–0.35PbTiO₃ (PIN-35PT), etc.^{21–24} Such softening of the velocity and the increase in the attenuation in the cubic phase are caused by the piezoelectric coupling of the strain polarization fluctuations in the non-centrosymmetric PNRs below the T_B .²⁵

The remarkable increase in the absorption coefficient of the LA mode towards $T_{C-T} = 308$ K was clearly observed as shown in Fig. 5. The plot of the sound attenuation shows the clear deviation at about 353 K from the constant temperature dependence at high temperatures as shown in the inset of Fig. 5. This temperature was assigned as the intermediate temperature (T^*) at which the rapid growth of PNRs begins. The increase in the LA mode absorption below the intermediate temperature indicates the start of rapid growth of the dynamic PNRs at T^* . A similar remarkable softening of C_{11} was reported in Ref. 26. When the reported density of 6078.65 kg/cm³ and the refractive index 2.33 (at the wavelength of 532 nm) of KTN40 are used,^{27,28} the observed values at 298 K are the elastic stiffness constant $C_{11} = 2.69 \times 10^{11}$ N/m², and $C_{44} = 0.97 \times 10^{11}$ N/m². The LA and TA

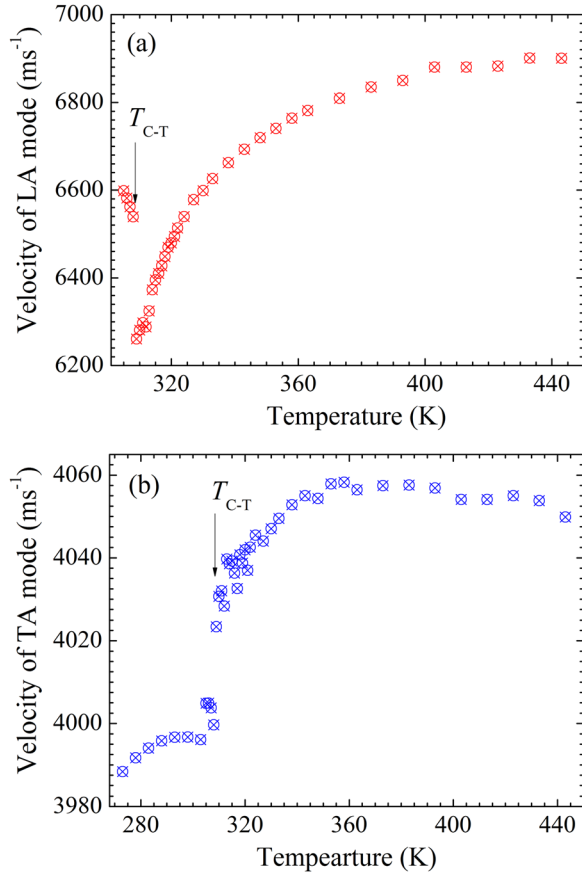


FIG. 4. The temperature dependences of (a) longitudinal velocity of the LA mode, and (b) transverse velocity of the TA mode in a KTN40 single crystal.

sound velocities are 6.65 km/s and 3.99 km/s, respectively. The values of the longitudinal sound velocity are in good agreement with the values of KTN32 reported in Ref. 11.

The mean-field theory of the sound attenuation anomaly was carried out by Landau and Khalatnikov and shows that this anomaly arises due to coupling between the strains and order parameter.²⁹ Based on the mean-field approximation, Levanyuk *et al.* found the temperature dependence of the

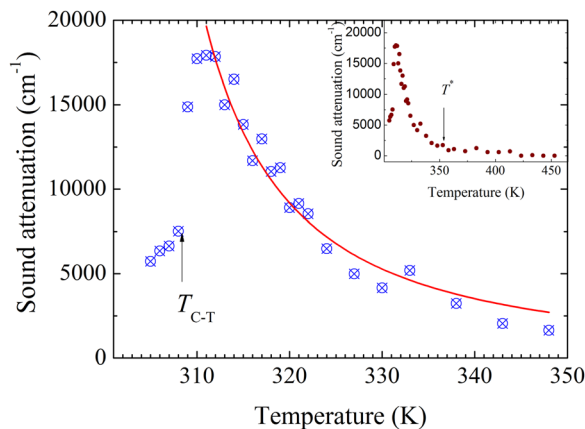


FIG. 5. Sound attenuation of a KTN40 single crystal as a function of temperature. The solid line indicates the curve fitted by Eq. (3). The inset shows the plot of large scale to show T^* .

sound attenuation in the following form with the critical exponent of 1.5 in the case of the order-disorder system³⁰

$$\alpha = \alpha_1(T - T_0)^{-n}. \quad (3)$$

In order to explain the anomalous behavior and order-disorder nature of the phase transition, we have fitted the sound attenuation between T_{C-T} and $T_{C-T} + 40$ K using Eq. (3). A good consistency between the experimental data and the fitting result was obtained with the exponent of 1.5, reflecting the order-disorder nature of the phase transition of the high quality KTN40 single crystals. The parameters obtained by fitting the sound attenuation are given in Table I. However, the observed sound attenuation is well fitted by the theoretical line, indicating that the anomaly arises due to coupling between the LA phonons and polarization fluctuations in the PNRs.

The critical slowing down is known as the typical phenomenon of the order-disorder phase transition. Currently, the diversive nature of the relaxation time of the polarization fluctuations in the ferroelectric phase transitions were observed by the broadband Brillouin scattering.^{23,25}

As shown in Fig. 3(b), the CP intensity increases with a decrease in temperature and its intensity becomes a maximum at T_{C-T} . The relaxation time was determined by the CP width Γ_{CP} using the following equation:²⁵

$$\pi\Gamma_{CP}\tau_{CP} = 1, \quad (4)$$

where τ_{CP} and Γ_{CP} are the relaxation time and width of the CP, respectively. The temperature dependence of the inverse relaxation time (Fig. 6) shows a linear dependence between T_{C-T} and 357 K, which indicates the fact that a cubic-tetragonal ferroelectric phase transition is the order-disorder type. The critical slowing down in the vicinity of T_{C-T} is given by

$$\frac{1}{\tau} = \frac{1}{\tau_0} + \frac{1}{\tau_1} \left(\frac{T - T_{C-T}}{T_{C-T}} \right). \quad (5)$$

In the temperature range of the cubic phase between T_{C-T} and $T_{C-T} + 49$ K, the observed values are $1/\tau_0 = 1.61 \times 10^{12} \text{ s}^{-1}$ and $1/\tau_1 = 1.48 \times 10^{11} \text{ s}^{-1}$. The value of τ_0 can be attributed to intrinsic lattice defects.³¹ Upon cooling, the CP intensity drastically increases toward T_{C-T} below T^* , indicating the rapid growth of the volume fraction of PNRs,⁸ which also induces the softening of the LA phonon velocity and the rapid increase in the attenuation from T^* to T_{C-T} .

We also studied the temperature dependence of the inverse of the susceptibility determined by the CP intensity and compared this result with the inverse dielectric constant as shown in Fig. 6(b). The intensity I_{CP} is related to the static susceptibility, $\chi(0)$, by the equation, $I = k_B T \chi(0)$, where k_B

TABLE I. Parameters obtained from fitting sound attenuation of a KTN40 single crystal.

$\alpha_1 (\times 10^6) (\text{cm}^{-1})$	T_0 (K)	n
1.03 ± 0.10	296.83 ± 1.05	1.5

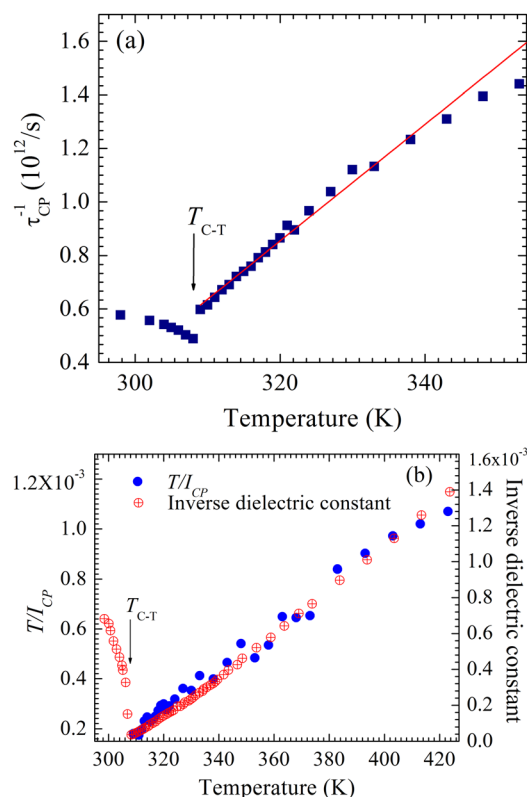


FIG. 6. The temperature dependence of (a) the inverse of the relaxation time determined from the CP width, where the solid line shown in (a) is result fitted using Eq. (5). (b) Temperature dependence of T/I_{CP} (closed circles) and the inverse dielectric constant (open circles) at the frequency of 1 kHz.

denotes the Boltzmann constant. The ratio of the slope just below and above T_{C-T} is about -3.2 , which is less than -2 (that for the second order transition). Therefore, this phase transition is slightly first order, which is in agreement with Courdille *et al.* and Triebwasser's for $x = 40\%$ and $x = 46\%$ crystals, respectively.^{32,33}

To discuss the temperature evolution of the dynamic nature of the PNRs, the average size of the dynamic PNRs was estimated by multiplying the relaxation time by the sound velocity of the LA mode because the maximum of the characteristics length of the strain fluctuations is given by the propagation length within the relaxation time.³⁴ Upon

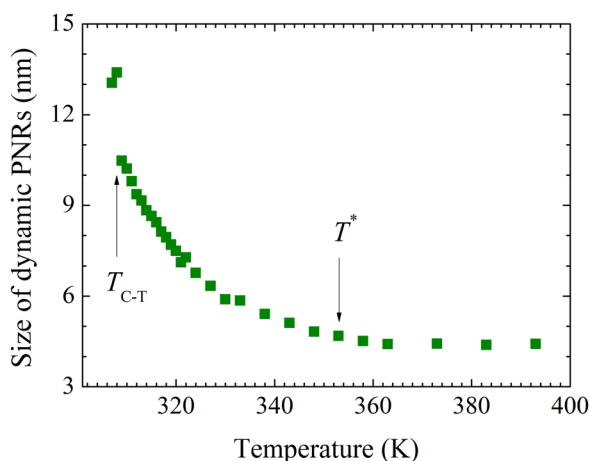


FIG. 7. The mean size of the dynamic PNRs as a function of temperature.

cooling, the average size of the dynamic PNRs increases toward T_{C-T} as shown in Fig. 7, reflecting the growth of the PNRs up to the percolation limit in which the reorientation is completely suppressed.³⁵ At an intermediate temperature T^* , the size is about 4.5 nm, which is in agreement with the size of a dynamic polar cluster of 4–6 nm.^{11,26}

IV. CONCLUSIONS

The relaxor-like dynamics related to PNRs have been investigated in the ferroelectric phase transition of $K(\text{Ta}_{1-x}\text{Nb}_x)\text{O}_3$ crystals with $x = 0.40$ using Brillouin and Raman scatterings. The local symmetry breaking caused by the PNRs in a paraelectric cubic phase was proved by the appearance of first-order Raman scattering with a polar rhombohedral symmetry. The remarkable softening of the velocity and the increase in attenuation of the LA mode were observed in the vicinity of the cubic-tetragonal ferroelectric phase transition temperature, $T_{C-T} = 308$ K. The increase in the LA mode attenuation was clearly observed below the intermediate temperature, $T^* = 353$ K, indicating the start of the rapid growth of the dynamic PNRs. The evolution of the dynamic PNRs was discussed based on the size growth with temperature, and below T^* , it rapidly increases towards T_{C-T} up to the percolation limit. The order-disorder nature of the ferroelectric phase transition is clearly observed by the critical slowing down towards T_{C-T} by the temperature variation of the broad central peaks. The soft mode behavior of KTN40 was not observed by Raman scattering. Therefore, it is concluded that the nature of the phase transition of KTN40 is purely order-disorder.

ACKNOWLEDGMENTS

This study was partly supported by a JSPS KAKENHI Grant. The authors thank Dr. T. H. Kim for his technical support of the Raman and Brillouin scattering measurements.

- ¹T. Imai, S. Yagi, S. Toyoda, J. Miyazu, K. Naganuma, S. Kawamura, M. Sasaura, and K. Fujiura, *Appl. Opt.* **51**, 1532 (2012).
- ²E. Dul'kin, S. Kojima, and M. Roth, *Euro. Phys. Lett.* **97**, 57004 (2012).
- ³E. Dul'kin, J. Petzelt, S. Kamba, E. Majaev, and M. Roth, *Appl. Phys. Lett.* **97**, 032903 (2010).
- ⁴G. Yong, J. Toulouse, R. Erwin, S. M. Shapiro, and B. Hennion, *Phys. Rev. B* **62**, 14736 (2000).
- ⁵J. Toulouse and R. Pattnaik, *J. Korean Phys. Soc.* **32**, S942 (1998).
- ⁶O. Svitelskiy and J. Toulouse, *J. Phys. Chem. Solids* **64**, 665 (2003).
- ⁷O. Hanske-Petitpierre, Y. Yakoby, J. Mustre De Leon, E. A. Stern, and J. J. Rehr, *Phys. Rev. B* **44**, 6700 (1991).
- ⁸J. P. Sokoloff, L. L. Chase, and L. A. Boatner, *Phys. Rev. B* **41**, 2398 (1990).
- ⁹A. Pashkin, V. Železný, and J. Petzelt, *J. Phys.: Condens. Matter* **17**, L265 (2005).
- ¹⁰J. Toulouse, P. DiAntonio, B. E. Vugmeister, X. M. Wang, and L. A. Knauss, *Phys. Rev. Lett.* **68**, 232 (1992).
- ¹¹R. Ohta, J. Zushi, T. Ariizumi, and S. Kojima, *Appl. Phys. Lett.* **98**, 092909 (2011).
- ¹²W. Kleemann, F. J. Schäfer, and D. Rytz, *Phys. Rev. Lett.* **54**, 2038 (1985).
- ¹³W. A. Bonner, E. F. Dearborn, and L. G. Van Uitert, *Am. Ceram. Soc. Bull.* **44**, 9 (1965).
- ¹⁴S. Kojima, *Jpn. J. Appl. Phys.* **49**, 07HA01 (2010).
- ¹⁵M. S. Islam, S. Tsukada, W. Chen, Z.-G. Ye, and S. Kojima, *J. Appl. Phys.* **112**, 114106 (2012).

- ¹⁶H. J. Trodahl, N. Klein, D. Damjanovic, N. Setter, B. Ludbrook, D. Rytz, and M. Kuball, *Appl. Phys. Lett.* **93**, 262901 (2008).
- ¹⁷S. K. Manlief and H. Y. Fan, *Phys. Rev. B* **5**, 4046 (1972).
- ¹⁸H. Taniguchi, M. Itoh, and D. Fu, *J. Raman Spectrosc.* **42**, 706 (2011).
- ¹⁹I. K. Jeong, T. W. Darling, J. K. Lee, T. Proffen, R. H. Heffner, J. S. Park, K. S. Hong, W. Dmowski, and T. Egami, *Phys. Rev. Lett.* **94**, 147602 (2005).
- ²⁰R. Vacher and L. Boyer, *Phys. Rev. B* **6**, 639 (1972).
- ²¹F. M. Jiang and S. Kojima, *Phys. Rev. B* **62**, 8572 (2000).
- ²²S. Kojima and J.-H. Ko, *Curr. Appl. Phys.* **11**, S22 (2011).
- ²³V. Sivasubramanian, S. Tsukada, and S. Kojima, *J. Appl. Phys.* **105**, 014108 (2009).
- ²⁴S. Kojima, S. Tsukada, Y. Hidaka, A. A. Bokov, and Z.-G. Ye, *J. Appl. Phys.* **109**, 084114 (2011).
- ²⁵S. Tsukada and S. Kojima, *Phys. Rev. B* **78**, 144106 (2008).
- ²⁶L. A. Knauss, X. M. Wang, and J. Toulouse, *Phys. Rev. B* **52**, 13261 (1995).
- ²⁷A. Reisman and E. Banks, *J. Am. Chem. Soc.* **80**, 1877 (1958).
- ²⁸F. S. Chen, J. E. Geusic, S. K. Kurtz, J. G. Skinner, and S. H. Wemple, *J. Appl. Phys.* **37**, 388 (1966).
- ²⁹L. D. Landau and E. M. Lifshitz, *Physical Kinetics* (Nauka, Moscow, 1979).
- ³⁰A. P. Levanyuk, S. A. Minyukov, and M. Vallade, *J. Phys. I France* **2**, 1949 (1992).
- ³¹A. Hushur, S. Gvasaliya, B. Roessli, S. Lushnikov, and S. Kojima, *Phys. Rev. B* **76**, 064104 (2007).
- ³²J. M. Courdile, J. Dumas, S. Ziolkiewicz, and J. Joffrin, *J. Phys. (Paris)* **38**, 1519 (1977).
- ³³S. Triebwasser, *Phys. Rev.* **114**, 63 (1959).
- ³⁴S. Kojima and S. Tsukada, *Ferroelectrics* **405**, 32 (2010).
- ³⁵R. Pirc and R. Blinc, *Phys. Rev. B* **76**, 020101 (2007).